Atomistic Simulation of Cracktip Failure Pathways in α-Fe

P.A. Gordon, T. Neeraj, Y. Li, and M.J. Luton

ExxonMobil Research & Engineering, Corporate Strategic Research
1545 Route 22 East, Annandale NJ, Peter.A.Gordon@exxonmobil.com

ABSTRACT

In this work, we present atomistic simulations with EAM potentials to identify the activated pathways and energetics for dislocation loop emission from an atomically sharp cracktip in single crsytal α-Fe. Nudged elastic band calculations are used to identify saddle-point transition states and energy barriers for dislocation emission at sub-critical stress intensities. From these calculations, the likely influence of these pathways on the ductile to brittle transition temperature is inferred.

Keywords: Iron, Steels, Simulation, Dislocation, Fracture

Introduction

The technological importance of fracture toughness and its temperature dependence, characterized by the brittle to ductile transition temperature (BDTT), is well known in the arena of high-strength steels development. For Fe and other BCC metals, which are generally viewed as intrinsically brittle materials, an increase in fracture toughness is observed over a relatively small temperature range.

A simple picture of the factors which influence the BDTT can be imagined with two interacting processes: dislocation nucleation from the cracktip region due to remote loading, described by the stress intensity factors K_I, K_{II}, and K_{III}, and convection (mobility) of emitted dislocations away from the cracktip region. Emitted dislocations from the crack contribute to elastic shielding, reducing the effective stress intensity at the tip. The mobility of dislocations away from the crack will alter the degree of shielding, which may change the apparent local cleavage toughness. If mobility is fast compared to dislocation generation, the BDTT should be nucleation controlled, while the opposite situation leads to a mobility controlled BDTT.

The extent to which these processes are controlling appears to be material dependent, and is still an active area of research. For instance, Roberts [1] has shown a close correspondence between the experimentally measured activation energies for the BDTT and the dislocation velocity for a number of materials, including silicon, germanium, and alumina. For these materials, this implies the importance of mobility in controlling the BDTT. However, it has also been shown in silicon that the sharpness of the transition is related to the spacing of dislocation sources near the cracktip; fewer sources lead to a more abrupt BDTT. By contrast, the work of Gumbsch et al [2] demonstrates that dislocation nucleation is important in the low temperature 'semi-brittle' regime in tungsten single crystals, although dislocation mobility appears to control the location of the BDTT. The nature of the dislocation sources, whether activated at or in the vicinity of the cracktip, is not clear from their studies. Furthermore, the activation energy for the BDTT is found to be much lower than the activation energy for glide of screw dislocations (0.2 vs 2 eV).

Recently, it has been shown that complex transition pathways can be explored in fully atomistic simulations using the nudged elastic band method [3]. In that work, emission of a dislocation loop from single crystal Cu was considered. While the activation energy reported in that work appears to be too high to be a likely pathway for emission, calculations were reported for only a single sub-critical stress intensity. The work suggests, however, that atomistic calculations can be a useful tool to probe the relationship between activation energy for the emission process as a function of applied stress intensity, whereby scaling laws for nucleation could be developed and parameterized in more coarse-grained models describing dynamic fracture.

In this work, we apply atomistic simulation, combined with an efficient approach for sampling transition pathways, to examine the activation energy barriers associated with cracktip blunting in model α-Fe. We illustrate the approach with two systems. First, we consider mode II loading of a crack with favorable orientation for edge emission on the slip plane ahead of the crack, and examine the activation pathways as a function of sub-critical stress intensity. We then consider mode I loading of a system that displays ductile emission in the athermal limit, and compare the likelihood of the emission pathway at the Griffith cleavage stress.

NSTI-Nanotech 2007, www.nsti.org, ISBN 1420061828 Vol. 1, 2007

Methods

In previous work [4], we performed extensive molecular statics calculations examining failure pathways of iron single crystals under mode I loading. The influence of crystallography, substitutional solutes, and sensitivity to the interatomic potential description was explored. On the basis of these results, we focus on two systems chosen for study, which are summarized in Table 1. The $(112)\langle 111\rangle$ crack plane/crack direction orientation under mode II loading was selected as a simple probe of the loop emission process. This orientation and loading mode is free of complicating effects such as the competitive failure mode of brittle cleavage and normal stress effects. The athermal response of the loading is emission of an edge dislocation on the crack plane ($\theta = 0°$). The $(110)\langle 001\rangle$ orientation under mode I loading was selected on the basis of our previous statics simulations; this orientation always resulted in ductile emission of an edge dislocation 54.7° from the crack plane for all potentials we considered.

Simulation cells representing the Fe single crystals contain roughly 500,000 atoms and are approximately $260\mathring{A}$ in the crack front (y) and crack propagation (x) directions. The crack front length is set at $40|\vec{b}|$, which is estimated to be sufficiently wide to accommodate nucleation of a dislocation loop [5] Interatomic interactions are governed by the Embedded Atom Method potential of Simonelli*et al* [6].

Cracks are inserted into the perfect crystal by the displacement field given by anisotropic LEFM. Several layers of atoms at the edge of the simulation cell are held fixed to enforce the elastic solution far away from the cracktip origin, while periodic boundary conditions are applied along the crack front direction. In the case of the mode II crack, several planes of atoms are removed behind the cracktip to prevent direct interactions between the cracktip surfaces.

Transition Pathway Methodology

A novel variant of the nudged elastic band method for transition pathway searching has been used in this work. The original method and variants proposed by Henkelman and Jonsson [7]–[9] has found widespread application in exploring reaction transition pathways, but becomes inefficient for strongly driven mechanical systems, where the transition from initial to final state results in a large release of stored elastic energy, and hence a large decrease in energy.

In the nudged elastic band method, a set of intermediate replica states are hypothesized, representing the system traversing the potential energy landscape between initial and final configurations. It is presumed that the starting and ending states represent local minima in the potential energy surface. If the replica is defined by the 3N dimensional vector $\vec{R}(3N)$, describing the atomic coordinates of the system, then a unit tangent vector $\vec{\tau}_i$, which marks the direction of the MEP at replica i, can be constructed as

$$\vec{\tau}_i \;=\; \frac{\vec{R}_i - \vec{R}_{i-1}}{|\vec{R}_i - \vec{R}_{i-1}|} + \frac{\vec{R}_{i+1} - \vec{R}_i}{|\vec{R}_{i+1} - \vec{R}_i|} \qquad (1)$$

To find the MEP, components of the force acting perpendicular to the local path direction, denoted as $\vec{F}_i|_\perp$, are minimized. In addition, to ensure that replicas maintain equal spacing across the entire path, a spring force $\vec{F}_{spring}$ with spring constant k is applied between adjacent replicas. The net force acting on a given replica to be minimized is

$$\vec{F}_{i,NEB} \;=\; \vec{F}_i|_\perp + (\vec{F}_{i,spring}\cdot\hat{\tau}_i)\hat{\tau}_i \qquad (2)$$

with

$$\vec{F}_i|_\perp \;=\; -\nabla E(\vec{R}_i) + (\nabla E(\vec{R}_i)\cdot\vec{\tau}_i)\vec{\tau}_i \qquad (3)$$

$$\vec{F}_{i,spring} \;=\; k(|\vec{R}_{i+1} - \vec{R}_i| - |\vec{R}_i - \vec{R}_{i-1}|) \qquad (4)$$

where ∇E represents the intermolecular forces acting on the atoms. These forces are applied to the intermediate replicas spanning the transition path, while the end point nodes remain fixed.

In the so-called free-end NEB treatment [10], the final node is no longer fixed, but is allowed to move on an isoenergy surface. This is accomplished by applying a force $\vec{F}_{free\ end}$ on the final node

$$\vec{F}_{free\ end} \;=\; \vec{F}_{spring} - \frac{(\vec{F}_{spring}\cdot\vec{F}_{end})\vec{F}_{end}}{|\vec{F}_{end}|^2} \qquad (5)$$

A spring connecting the end node to its neighbor is purely repulsive ($\vec{F}_{spring} = k(|\vec{R}_n - \vec{R}_{n-1}|)$), and serves to keep spacing between the adjacent replica. The second term in eq 5 is the projection of this spring force in the direction of the interatomic forces; subtraction of this from the original spring force results in a force perpendicular to the interatomic forces, a net force that moves the replica on a constant energy surface. This allows one to examine a subset of the total transition pathway by replacing the final node configuration with a replica that is closer to the region of interest, such as near, but over, the transition state barrier.

Results

Mode II Loading

The result of a typical free-end NEB calculation is shown in Figure 1. The system shown is at a sub-critical stress intensity of $K_{II} = 0.40MPa\sqrt{m}$. The figure shows the MEP of the loop emission pathway. The activation energy barrier for this path is approximately 0.9

Table 1: Summary of orientations considered for transition pathway analysis.

Crack Orientation (plane)[direction]	Loading Mode	Slip System	θ degrees	$K_{i,athermal}$ MPa$\sqrt{m}$
(110)[001]	I	$\{112\}\langle 111\rangle$	± 54.7	0.96
(112)[111]	II	$\{112\}\langle 111\rangle$	0	0.53

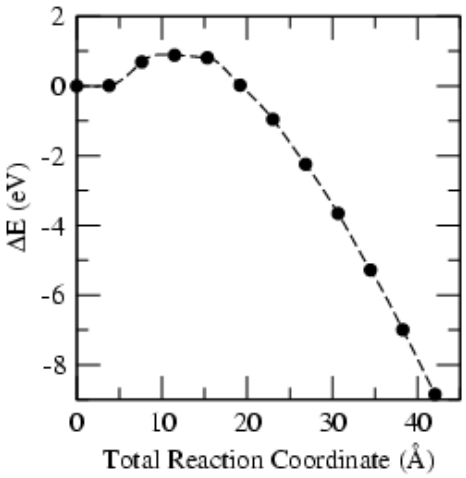

Figure 1: Minimum energy path obtained for loop nucleation in NEB calculation for $\{112\}\langle 111\rangle$ crack at $K_{II} = 0.40MPa\sqrt{m}$.

eV. Configurations along the minimum energy path at the transition state and for the free-end configuration at the end of the calculation are also depicted in Figure 2. The features of the loop appear qualitatively similar to hybrid continuum/interplanar potential models [11] and atomistic simulations [3].

Similar calculations have been performed over a range of sub-critical stress intensities. As expected, the critical loop nucleus and activation energy at the transition state decreases with increasing stress intensity. Below a stress intensity of ≈ 0.32 MPa$\sqrt{m}$, the apparent critical loop nucleus width exceeds half the simulation cell thickness along the crackfront, suggesting that system size effects may influence the results at this size. The scaling of the activation energies may be expressed as a function of sub-critical stress intensity,

$$\Delta E_{act} \propto (K_{II}^{ath} - K_{II})^n \qquad (6)$$

The loop activation energy scales to exponent n=3.0.

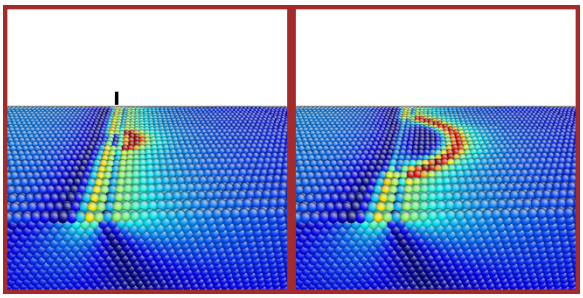

Figure 2: Resolved shear stress distributions along slip plane of selected replicas along minimum energgy path for loop emission under mode II loading at $K_{II} = 0.40MPa\sqrt{m}$. Magnitude of stress color coded from blue (low) to red (high). Left: transition state, right: free-end replica.

Mode I Loading

The activation energies obtained as a function of mode I loading of the $(110)\langle 001\rangle$ crack is shown in Figure 3. A fit of eq 6 to this data yields a scaling exponent of 2.6, in reasonable agreement with the previous example. Qualitatively, the loop emission process is similar to the mode II nucleation, although there are more pronounced normal stresses along the dislocation embryo boundary in this mode. The NEB calculations had more difficulty converging at loads above the Griffith stress intensity ($K_{I,Gr} = 0.865$ MPa$\sqrt{m}$). This may be due to the fact that the competing failure pathway of brittle cleavage is present. [1]

Given the activation energies obtained, we can estimate the frequency, ν, of loop nucleation due to external perturbations following the approach of Rice and Beltz [14],

$$\nu = n(\frac{c_{shear}}{b})exp(\frac{-\Delta E(K_I)}{kT}) \qquad (7)$$

[1] It is worth noting that several Fe potentials, notably those developed by Ackland *et al*[12] and Mendelevet al[13] exhibit both brittle *and* ductile failure in similar statics simulations, depending on the precise origin of the inserted crack. This suggests that, for this orientation, the brittle and ductile failure pathways in these model materials must be energetically similar. This is in contrast to many previous simulation studies in Cu or Si, which probe ductile *or* brittle pathways where the failure pathway is evidently tilted strongly in favor of a single response.

NSTI-Nanotech 2007, www.nsti.org, ISBN 1420061828 Vol. 1, 2007

where $\frac{c_{shear}}{b}$ represents the attempt frequency of activated nucleation, and n represents the number of nucleation sites per unit length of crackfront.

Taking the shear wave speed as $\approx 3\frac{km}{s}$, and n as the inverse of the critical loop width at a given value of K_I, we can estimate the nucleation frequency as a function of applied stress intensity. For example, at the Griffith stress and room temperature, the nucleation rate is $\approx 10^{10}$ events per mm crackfront per second. Following Rice, assuming a lower bound frequency of $10^6(s.mm)^{-1}$ is necessary to be observable on a laboratory timescale, this nucleation pathway should be expected to operate with ease for a dynamically (overloaded?) moving crack. This seems consistent with the observations of Odette *et al* who found evidence of emission in the dynamic fracture of (110) cracks in single crystal Fe[15]. Furthermore, at 300K, the nucleation process should be observable above $\frac{K_I}{K_{I,ath}} \approx 0.86$, which compares favorably to the Rice and Beltz estimate of 0.90-0.95.

Over the temperature range of 250-350K, a typical span over which the fracture toughness of Fe goes from brittle to ductile, we estimate that the nucleation rate increase nearly 4 orders of magnitude at K_{Gr}. The magnitude of the frequency rise with temperature increases with decreasing K_I, however, it seems clear that in the range of stresses near the Griffith stress intensity, the emission process should change from a relatively infrequent to frequent event.

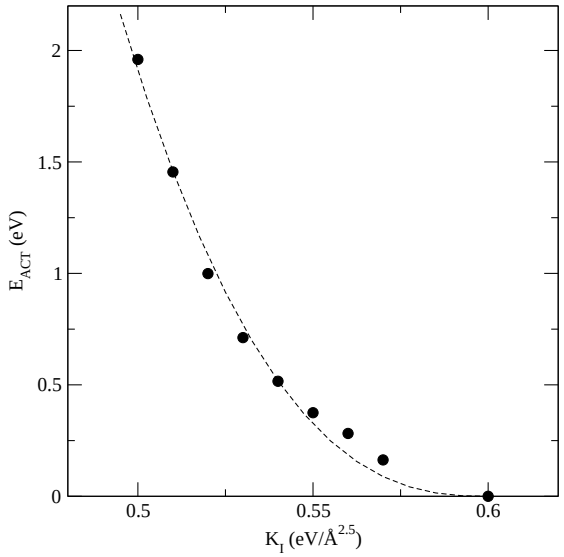

Figure 3: Activation energy for loop emission vs. mode I stress intensity. Dotted line is best fit to loop activation energy data.

REFERENCES

[1] S.G. Roberts. Modelling the brittle to ductile transition in single crystals. In *NATO ASI Series, Series E: Applied Sciences*, volume 308, pages 409–433, 1996.

[2] P. Gumbsch, J. Riedle, A. Hartmaier, and H.F. Fischmeister. *Science*, 282:1293–1295, 1998.

[3] T. Zhu, J. Li, and S. Yip. *Phys. Rev. Lett.*, 93:025503–1–4, 2004.

[4] P.A. Gordon, T. Neeraj, and M.J. Luton. *Met. and Mat. Trans. A*, 37a:xxx, 2006.

[5] G. Xu, A. S. Argon, and M. Ortiz. *Phil. Mag. A*, 72:415–451, 1995.

[6] G. Simonelli, R. Pasianot, and E.J. Savino. *Materials Research Society Symposium Proceedings*, 291:567–572, 1993.

[7] G. Henkelman and H. Jonsson. *J. Chem. Phys.*, 113:9978–9985, 2000.

[8] G. Henkelman, B. P. Uberuaga, and H. Jonsson. *J. Chem. Phys.*, 113:9901–9904, 2000.

[9] G. Henkelman and H. Jonsson. *J. Chem. Phys.*, 111:7010–7022, 1999.

[10] J. Li and P.A. Gordon T. Zhu. *Mod. Sim. Mater. Sci. Eng.* to be submitted.

[11] G. Xu, A. S. Argon, and M. Ortiz. *Phil. Mag. A*, 75:341–367, 1997.

[12] G. J. Ackland, D. J. Bacon, A. F. Calder, and T. Harry. *Philosophical Magazine A*, 75(3):713–732, 1997.

[13] M. I. Mendelev, S. Han, D. J. Srolovitz, G. J. Ackland, D. Y. Sun, and M. Asta. *Philosophical Magazine*, 83(35):3977–3994, 2003.

[14] J.R. Rice and G.E. Beltz. *J. Mech. Phys. Sol.*, 42:333–360, 1994.

[15] M.L. Hribernik. *Cleavage Oriented Iron Single Crystal Fracture Toughness.* PhD thesis, University of California Santa Barbara, 2006.